Peroxynitrite-Mediated τ Modifications Stabilize Preformed Filaments and Destabilize Microtubules through Distinct Mechanisms†

Matthew R. Reynolds,*,‡ Thomas J. Lukas,§ Robert W. Berry,‡,|| and Lester I. Binder‡,||

Department of Cell and Molecular Biology, Department of Molecular Pharmacology and Biological Chemistry, and Cognitive Neurology and Alzheimer's Disease Center, Feinberg School of Medicine, Northwestern University, Chicago, Illinois 60611

Received October 20, 2005; Revised Manuscript Received January 24, 2006

ABSTRACT: Alzheimer's disease (AD) is a progressive amnestic dementia typified by abnormal modifications of the microtubule (MT)-associated τ protein that promote its pathological self-assembly and displacement from the MT lattice. Previously, we showed that peroxynitrite ($ONOO^-$) induces the oxidative 3,3′-dityrosine (3,3′-DT) cross-linking and site-selective nitration of τ monomers [Reynolds et al. (2005) *Biochemistry 44*, 1690−1700]. In the present study, we examined the effects of $ONOO^-$-mediated modifications on two key elements of τ pathobiology: (1) the stability of preformed τ filaments and (2) the ability of monomeric τ to promote tubulin assembly. Here, we report that treatment of synthetic τ filaments with $ONOO^-$ generates heat-stable, SDS-insoluble aggregates with a significantly reduced mobility by SDS−PAGE compared to that of nontreated filaments. Ultrastructurally, these aggregates appear to be cross-linked via interfilament bridges. Using LC−MS/MS and HPLC with fluorescent detection, we demonstrate that covalent 3,3′-DT linkages are present within these higher-order aggregates. Similar to monomeric τ, filamentous τ exhibits a hierarchical pattern of nitration following $ONOO^-$ treatment with site selectivity toward the amino-terminal residues Tyr18 and Tyr29. Further, select nitration of residues Tyr18, Tyr29, Tyr197, and Tyr394, events known to stabilize the pathological Alz-50 conformation [Reynolds et al. (2005) *Biochemistry 44*, 13997−14009], inhibits the ability of monomeric τ to promote tubulin assembly. This effect is specific for the 3-NT modification, as mutant τ proteins pseudophosphorylated at each Tyr residue are fully competent to stabilize MTs. Collectively, our results suggest that $ONOO^-$-mediated modifications stabilize τ filaments via 3,3′-DT bonding and destabilize MTs by site-selective nitration of τ monomers. Moreover, assumption of the Alz-50 conformation may be the mechanism through which τ nitration modulates MT stability.

Alzheimer's disease (AD)[1] is a progressive neurodegenerative disorder and the most common cause of dementia in the elderly. Clinically, AD manifests as an insidious deterioration of mental function affecting memory and one or more cognitive domains (*1*). Pathologically, the signatures of postmortem AD brain include neurofibrillary tangles (NFT), neuritic plaques, and neuropil threads. The NFT is largely composed of the MT-associated τ protein assembled into paired helical filaments (PHF) and straight filaments (SF) (*2*−*6*). The neuritic plaques surround extracellular deposits of the β-amyloid (Aβ) peptide (*7*). Of these lesions, cognitive decline correlates most closely with the regional distribution of NFTs (*8*). In addition, mutations in the τ gene define a heterogeneous group of frontal lobe dementias (*9*−*11*), providing strong genetic evidence that τ dysfunction alone is sufficient for neurodegeneration. While Aβ aggregates are damaging to neurons in several model systems (*12*−*14*), τ appears to be a prerequisite for this effect, as τ-deficient neurons are resistant to Aβ-induced neurotoxicity (*15*).

τ is a natively unfolded protein in solution dominated by random coil structure (*16*, *17*). During aggregation, however, certain regions of the τ molecule become highly ordered and assume a β-pleated sheet conformation (*18*−*20*). Abnormal modifications of τ, including phosphorylation (*21*−*23*), truncation (*24*), and conformational changes (*25*−*27*), are thought to play an important role in the series of events leading to NFT formation. In fact, work from our own laboratory has demonstrated that τ undergoes a series of conformational changes during the course of tangle evolution. For example, in early-stage tangles, the extreme amino

† This work was supported by NIH Grants AG 14453 (L.I.B.), AG 21184 (L.I.B.), and F30 NS051043 (M.R.R.).

* To whom correspondence should be addressed: Feinberg School of Medicine, Northwestern University, Tarry Building 8-754, 303 E. Chicago Ave., Chicago, IL 60611. Phone: (312) 503-0824. Fax: (312) 503-7912. E-mail: m-reynolds@md.northwestern.edu.

‡ Department of Cell and Molecular Biology.

§ Department of Molecular Pharmacology and Biological Chemistry.

|| Cognitive Neurology and Alzheimer's Disease Center.

[1] Abbreviations: ArA, arachidonic acid; AAA, amino acid analysis; ACN, acetonitrile; AD, Alzheimer's disease; 3,3′-DT, 3,3′-dityrosine; DTPA, diethylenetriaminepentaacetic acid; DTT, dithiothreitol; EDTA, ethylenediaminetetraacetic acid; EGTA, ethylene glycol bis(β-aminoethyl ether)-*N*,*N*,*N*′,*N*′-tetraacetic acid; ESI-MS, electrospray ionization mass spectrometry; GTP, guanosine triphosphate; HEPES, *N*-(2-hydroxyethyl)piperazine-*N*′-ethanesulfonic acid; HPLC, high-performance liquid chromatography; MAP, microtubule-associated protein; MES, 2-(*N*-morpholino)ethanesulfonic acid; MT, microtubule; MTBR, microtubule-binding repeat; NFT, neurofibrillary tangle; 3-NT, 3-nitrotyrosine; $ONOO^-$, peroxynitrite; PD, Parkinson's disease; PHF, paired helical filament; PIPES, piperazine-*N*,*N*′-bis(2-ethanesulfonic acid); PMSF, phenylmethanesulfonyl fluoride; SDS−PAGE, sodium dodecyl sulfate−polyacrylamide gel electrophoresis; SEM, standard error of the mean; SF, straight filament; TFA, trifluoroacetic acid.

10.1021/bi052142h CCC: $33.50
Published on Web 03/08/2006

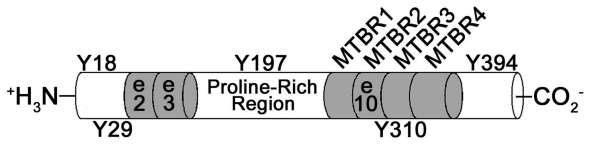

FIGURE 1: Structure of full-length human τ (hτ40). Human τ proteins are encoded by a single gene on chromosome 17p21 (*68*). Alternative splicing of exons 2, 3, and 10 yields six central nervous system isoforms that differ in the number of amino-terminal insertions and tandem MT-binding repeats (MTBR). The five Tyr residues in hτ40 are located at positions Tyr18, Tyr29, Tyr197, Tyr310, and Tyr394 (numbering according to ref *70*).

terminus of τ comes into close apposition with the third MT-binding repeat (MTBR3) (Figure 1). This event accompanies early filamentous changes in τ and is detected by the conformation-dependent antibody Alz-50 (*28*, *29*). In middle- to late-stage tangles, amino- and carboxy-terminal truncations drive the formation of the Tau-66 conformation (*25*−*27*). Further modifications of the Tau-66 arrangement yield the primary building blocks of the PHF core (*30*−*32*). These findings suggest that, during the course of AD, τ undergoes an ordered sequence of conformational rearrangements that promote its misfolding and deposition.

Neuroinflammation and oxidative injury are pervasive features of Alzheimer's brain (reviewed in ref *33*). During Aβ-associated inflammation, reactive nitrogen and oxygen species are generated that can cause neuronal dysfunction and death (*34*−*37*). Prevalent among these species is peroxynitrite ($ONOO^-$), a powerful in vivo oxidant capable of lipid peroxidation (*38*), DNA damage (*39*−*42*), inactivation of metalloenzymes (*43*−*46*), and protein nitration and/or oxidation (*47*). Substantial evidence supports the role of $ONOO^-$ as the principal in vivo nitrating agent (*48*−*50*). $ONOO^-$ is generated from the near-diffusion-limited reaction of nitric oxide and superoxide radicals (*51*). Covalent modification of proteins may then occur from the addition of a 3-nitrotyrosine (3-NT) group onto the Tyr phenolic ring. Importantly, nitration occurs with biological selectivity and can significantly influence protein function (*52*−*56*). In addition to its nitrative role, $ONOO^-$ can cross-link proteins through the formation of 3,3′-DT linkages (*57*, *58*).

Five Tyr residues, located at positions Tyr18, Tyr29, Tyr197, Tyr310, and Tyr394, span the length of the human τ protein (Figure 1). While six central nervous system isoforms are generated from alternative splicing of the τ message, all five Tyr residues are equally represented in each isoform (*59*−*61*). Importantly, these Tyr residues are positioned within functionally relevant regions of the τ protein. For example, two of these residues, Tyr18 and Tyr29, are sequestered within the extreme amino terminus of τ. This region of the τ molecule lacks significant secondary structure (*62*) and is highly accessible to the bulk solvent, even when τ is bound to the MT surface (*63*). Significantly, removal of the extreme amino terminus inhibits τ polymerization in vitro (*62*). This latter finding supports a facilitative role for the amino terminus in τ assembly, likely by its contribution to the Alz-50 conformation. In contrast, Tyr197 resides within the proline- and glycine-rich interior of τ. This region is believed to impart the flexibility and molecular spacing necessary for dynamic conformational events to occur (*64*, *65*). Tyr310 is part of a critical interaction motif (^{306}VQIVYK^{311}) in MTBR3 that is known to be essential for in vitro τ assembly (*19*). In addition to its role in MT binding, this region of τ comprises the minimal protease-resistant unit of the PHF (*66*). Adjacent to the carboxy terminus of τ lies Tyr394. The carboxy terminus is believed to protect against τ filament formation by folding back upon the MTBR region and sterically preventing the Alz-50 conformation (*67*).

One canonical model of τ-induced neurodegeneration proposes that abnormal τ modifications render the protein structurally permissive to aggregation. The resulting τ aggregates then confer a toxic gain-of-function effect that directly compromises neuronal viability. Another, equally attractive, theory is based upon the physiological role of τ in binding and stabilizing the MT network (*63*). In this loss-of-function paradigm, abnormal τ modifications displace τ from the MT surface (*68*). This event, in turn, destabilizes MT-based axonal transport, prevents the delivery of vital cellular cargo, and, eventually, culminates in neuronal death.

Based upon these two models of τ dysfunction in AD, we examined the effects of $ONOO^-$-mediated τ modifications on filament stability and MT stabilization. The results presented herein are the first to definitively demonstrate that $ONOO^-$ treatment of τ stabilizes preformed filaments and inhibits the binding of monomeric τ to MTs through distinct mechanisms. Stabilization and/or aggregation of τ filaments occurs via oxidative 3,3′-DT cross-linking, whereas MT destabilization results from select nitration of τ monomers. Intriguingly, τ mutants that mimic phosphorylation at each Tyr residue are fully competent to support tubulin assembly. This latter finding suggests that τ nitration specifically disrupts MT binding. Further, since nitrative modification at residues Tyr18, Tyr29, Tyr197, and Tyr394 stabilizes the Alz-50 conformation (*69*), our data reveal that the Alz-50 epitope may prevent τ−MT interactions. Taken together, these results provide a novel mechanism for how neuroinflammatory sequelae can stabilize τ aggregates and alter the neuronal cytoskeleton in Alzheimer's brain.

EXPERIMENTAL PROCEDURES

Mutagenesis, Expression, and Purification of hτ40. Wild-type and mutant τ proteins were expressed in *Escherichia coli* strain BL21 (DE3) [F^- *omp*T *hsd*S_B ($r_B^-m_B^-$) *gal dcm*] cells using the pT7C-hτ40 plasmid. This plasmid drives high-level expression of full-length human τ (hτ40) fused to an amino-terminal six-His affinity tag (*28*). The hτ40 cDNA harbors the longest central nervous system isoform of τ (441 residues) containing two amino-terminal insertions as well as alternatively spliced exons 2, 3, and 10 (*70*). Genetic modifications of the pT7C-hτ40 plasmid were introduced using a site-directed mutagenesis kit (Stratagene) with 33−38-mer oligomers (Integrated DNA Technologies, Inc.) that define the sequence flanking each targeted codon. Multiple rounds of Tyr → Phe mutagenesis were used to generate quadruple hτ40 mutants that contain single Tyr residues at each position in the native hτ40 protein (Tyr18, Tyr29, Tyr197, Tyr310, and Tyr394). The nomenclature and description of all Tyr → Phe hτ40 mutants, both nitrated and nonmodified, have been presented previously (*69*, *71*). For example, the quadruple hτ40 mutant containing a single Tyr residue at position Tyr18 (i.e. $^{Y}29^{F}$, $^{Y}197^{F}$, $^{Y}310^{F}$, and $^{Y}394^{F}$) is denoted as ^{18}Y. The nitrated variant of this same

^{18}Y mutant is designated as ^{18}nY. A quintuple hτ40 mutant lacking all Tyr residues, termed ^{5x}Y→F, was engineered to serve as a negative control for nitration. Additionally, five Tyr → Glu pseudophosphorylation mutants were designed to mimic phosphorylation at each Tyr residue (*71*). The identity and position of all mutations were confirmed by automated DNA sequencing (Center for AIDS Research DNA Sequencing Core, Northwestern University, Chicago, IL). Wild-type and mutant hτ40 proteins were purified over a Ni−NTA metal affinity column (Qiagen) (*72*, *73*). Size-exclusion chromatography was subsequently performed to isolate full-length hτ40 from incompletely translated hτ40 proteins that retain the six-His affinity tag (*73*).

Nitration of Mutant hτ40 Proteins. $ONOO^-$ was prepared from sodium nitrite and acidified H_2O_2 as described previously (*74*). Residual H_2O_2 was removed by passing the $ONOO^-$ stock solution over a manganese dioxide column (*75*). The $ONOO^-$ concentration was determined spectrophotometrically at 320 nm in 0.3 M NaOH (ϵ_{302} = 1670 M^{-1} cm^{-1}) preceding each experiment (*53*). Wild-type and mutant hτ40 proteins were dialyzed against nitration buffer [100 mM potassium phosphate, 25 mM sodium bicarbonate (pH 7.4), and 0.1 mM diethylenetriaminepentaacetic acid (DTPA)] for 16 h at 4 °C. Postdialysis protein concentrations were determined by the Lowry method using bovine serum albumin as a standard (*76*). A 100-fold molar excess of $ONOO^-$ was added to each mutant protein in two boluses with vigorous stirring for 30 s at room temperature. The final pH of the solution was measured and kept at 7.4 (*77*). Following $ONOO^-$ treatment, proteins were concentrated via Centriprep YM-10 filter devices (Millipore) and purified over a Sephacryl S-300 gel filtration column (Amersham Biosciences) to separate nitrated hτ40 monomers from 3,3′-DT cross-linked hτ40 oligomers (*69*, *71*). Protein purity was assessed by sodium dodecyl sulfate−polyacrylamide gel electrophoresis (SDS−PAGE) with Coomassie Brilliant Blue staining. Final concentrations of nitrated, monomeric hτ40 proteins were again determined by the Lowry method using bovine serum albumin as a standard (*76*).

Amino Acid Analyses of Nitrated Mutant hτ40 Proteins. Amino acid analyses (AAA) were performed to characterize the percentage of nitrated versus nonnitrated hτ40 in each mutant protein preparation. Briefly, nitrated mutant hτ40 proteins were subjected to vapor-phase hydrolysis via treatment with 6 N HCl and 0.1% phenol at 110 °C for 24 h. The hydrolysates were dried under vacuum, resuspended in 0.1% formic acid, and separated by ion-exchange chromatography. AAA was performed using a Hitachi L-8800 instrument equipped with a sodium citrate buffer system. A mononitrated L-Tyr standard (Sigma) was fully resolved from Phe and L-Tyr in the chromatography system. Two-point external calibration was utilized in all experiments.

Polymerization Reactions. Polymerization of hτ40 was induced using arachidonic acid (ArA) as described previously (*78*). A working solution of ArA was prepared by diluting a 100 mg/mL stock (Cayman Chemicals) in 100% ethanol to a final concentration of 2 mM. All working ArA solutions were discarded immediately after use, and stock solutions were stored at −20 °C for no longer than 1 month to prevent oxidation. Wild-type and mutant hτ40 proteins were diluted into polymerization buffer [10 mM *N*-(2-hydroxyethyl)-piperazine-*N*′-ethanesulfonic acid (HEPES) (pH 7.4), 100 mM NaCl, and 5 mM dithiothreitol (DTT)] to a final concentration of 4 μM. It was previously demonstrated that the amino-terminal affinity tag has no effect on hτ40 polymerization in vitro (*65*). Polymerization was initiated by adding the ArA inducer to a final concentration of 75 μM. Reaction solutions were incubated for 6 h at room temperature without stirring. Polymerization progress was monitored by right-angle laser light scattering and transmission electron microscopy (EM).

Treatment of Wild-Type and Mutant hτ40 Filaments with $ONOO^-$. Wild-type and mutant hτ40 filaments, assembled as described in detail above, were centrifuged at 100000*g* for 1 h in a type 70.1 Ti rotor (Beckman). Following aspiration of the soluble hτ40 monomers, the sedimented hτ40 filaments were washed twice with nitration buffer and then resuspended in 50−100 μL of nitration buffer. A 100-fold molar excess of $ONOO^-$ was added to each sample in two boluses with vigorous stirring for 30 s at room temperature. The final pH of the solution was measured and kept at 7.4 (*77*).

Filament Stability Assays. Nonmodified and $ONOO^-$-treated wild-type filaments were prepared as described above. Samples were boiled for 10 min in Laemmli sample buffer [0.125 M Tris (pH 6.8), 4% SDS, 20% glycerol, and 10% β-mercaptoethanol], resolved electrophoretically on a one-dimensional polyacrylamide gel, and stained using the Coomassie Brilliant Blue reagent. Gels were scanned, saved as .tif files, and imported into Adobe Photoshop version 7.0 for image processing.

Transmission Electron Microscopy. Nonmodified and $ONOO^-$-treated wild-type filaments were fixed in 2% (w/v) glutaraldehyde for transmission EM analysis. Briefly, samples were absorbed onto 300-mesh, carbon-coated Formvar grids (Electron Microscopy Sciences), negatively stained using 2% (w/v) uranyl acetate, and analyzed using the JEOL JEM-1220 EM instrument at 60 kV and a magnification of 20000× (*79*). Images were captured using a digital camera (Kodak MegaPlus model 1.6I AMT) controlled by the AMT Camera Controller software package. For each experiment, grids were prepared in triplicate and filament morphology was assessed from six random images per grid (*65*). Digital electron micrographs were processed in Adobe Photoshop version 7.0 where the brightness and contrast were adjusted to optimize visualization (*67*).

Characterization of 3,3′-DT in $ONOO^-$-Treated Filaments. Wild-type hτ40 proteins (25−30 mg) were polymerized in the presence of ArA as detailed above. Following a 16 h incubation, a reaction aliquot was removed and processed for transmission EM to verify filament formation. The reaction mixture was centrifuged at 100000*g* for 1 h, and the resultant pellet was resuspended in 0.5−1.0 mL of nitration buffer. The filamentous suspension was treated with a 100-fold molar excess of $ONOO^-$ and passed over a Sephacryl S-300 gel filtration column (Amersham Biosciences) to separate higher-order hτ40 aggregates (>250 kDa) from monomeric (68 kDa) and filamentous (∼250 kDa) hτ40 species (*73*). Each of these hτ40 fractions was hydrolyzed into their constituent amino acids by reaction with 6 N HCl at 110 °C for 16 h under argon. The hydrolysates were dried under vacuum, resuspended in 0.1% trifluoroacetic acid (TFA), and separated on a Platinum C_{18} reverse-phase column (5 μm, 300 Å, 250 mm × 4.6 mm, Alltech)

at a rate of 1 mL/min. High-performance liquid chromatography (HPLC) was performed on a HP 1100 system (Hewlett-Packard) using a linear gradient of 0 to 15% acetonitrile (ACN) containing 0.1% TFA over the course of 30 min. Eluates were monitored by their ultraviolet absorbance at 215 nm and their fluorescent emission profile (λ_{ex} = 283 nm, λ_{em} = 410 nm). L-Tyr, 3,3′-DT, and 3-NT were identified by their coelution with external standards. The 3,3′-DT standard was synthesized by reacting horseradish peroxidase with L-Tyr and H_2O_2 as described previously (*77*).

Electrospray ionization mass spectrometry (ESI-MS) was performed on a 1100 LC/MSD Trap XCT system (Agilent Technologies) equipped with an electrospray source operating in the positive ion acquisition mode. The hydrolysates were resolved on a Platinum C_{18} reverse-phase column (5 μm, 300 Å, 250 mm × 4.6 mm, Alltech) at a flow rate of 400 μL/min. An increasing linear gradient from 0 to 15% ACN containing 0.1% formic acid was used to resolve the reaction products. The ESI-MS conditions were as follows: capillary temperature of 325 °C, nitrogen sheath gas pressure of 18 psi, and ion spray voltage of 2.5 kV. Tandem MS/MS scans were performed to further characterize the L-Tyr, 3-NT, and 3,3′-DT products. Multipoint external calibration was employed for all mass spectra.

Mapping Nitration Sites in Mutant hτ40 Filaments. Solid-phase dot blot assays were performed as described (*28*) to measure 3-NT immunoreactivity in nitrated wild-type and nitrated mutant hτ40 filaments. Briefly, $ONOO^-$-treated wild-type and mutant hτ40 filaments were isolated from residual hτ40 monomers using YM-100 centrifugal filter devices (Millipore). The nitrated filaments were diluted to a final concentration of 5 ng/μL in wash buffer [100 mM boric acid, 2.0 mM sodium borate decahydrate, 75 mM NaCl, 0.05% (w/v) thimerosal, 0.4% (w/v) bovine serum albumin, and 0.05% (w/v) Tween 20], and 1 μL of sample was adsorbed onto a 0.45 μm nitrocellulose membrane (Whatman). Membranes were dried for 1 h at 37 °C, blocked for 1 h in a 5% (w/v) solution of nonfat dry milk, and incubated for 16 h at 4 °C in a polyclonal 3-NT (1 μg/mL; Chemicon) or monoclonal Tau-5 (20 ng/mL) antibody solution. Following a secondary incubation with a horseradish peroxidase-conjugated anti-rabbit or anti-mouse antibody (Jackson ImmunoResearch), the membranes were developed using enhanced chemiluminescence (Amersham Biosciences) and exposed to autoradiographic film. Signal intensities from each sample were quantified using Scion Image software. A standard curve was included in each experiment to ensure that the signal intensities fell within the linear range of the assay. Subsequently, the autoradiograph exposures were imported into Photoshop version 7.0 where the brightness and contrast were adjusted to optimize visualization.

Previously, we showed that the polyclonal 3-NT antibody cross-reacts to a moderate degree with nonmodified hτ40 (*69*, *71*). For this reason, the signal due to cross-reactivity of the 3-NT antibody with wild-type hτ40 filaments was subtracted from all measurements. The level of statistical significance was set at 0.05, and means were compared using the Student's two-tailed *t* test.

Tubulin Purification. Tubulin was purified from porcine brain extracts as described previously (*80*). Briefly, fresh porcine brains, generously donated by a local slaughterhouse (Park Packing Co., Chicago, IL), were homogenized in 0.5 mL/g polymerization buffer [0.1 M piperazine-*N*,*N*′-bis(2-ethanesulfonic acid) (PIPES) (pH 6.8), 0.5 mM $MgCl_2$, 2.0 mM ethylene glycol bis(β-aminoethyl ether)-*N*,*N*,*N*′,*N*′-tetraacetic acid (EGTA), 0.1 mM ethylenediaminetetraacetic acid (EDTA), 0.1% (v/v) β-mercaptoethanol, 1.0 mM adenosine triphosphate (ATP), and 1.0 mM phenylmethanesulfonyl fluoride (PMSF)]. Microtubule-associated protein (MAP)-free tubulin was purified by one temperature-dependent polymerization/depolymerization cycle, centrifugation over a 40% glycerol cushion [0.5 mM PIPES (pH 6.8), 0.5 mM $MgCl_2$, 2.0 mM EGTA, 0.1 mM EDTA, 40% (w/v) glycerol, 0.1% (v/v) β-mercaptoethanol, 1.0 mM ATP, and 1.0 mM PMSF], and phosphocellulose chromatography. Tubulin aliquots were snap-frozen in liquid nitrogen and stored at −80 °C. The concentration of tubulin was determined by SDS−PAGE with quantitative Coomassie Brilliant Blue staining.

τ-MT Cosedimentation Assays. Phosphocellulose-purified tubulin (10 μM) was copolymerized with wild-type, nitrated wild-type, nitrated mutant, or pseudophosphorylated hτ40 (2 μM) in PMEM buffer [87 mM PIPES (pH 6.8), 36 mM 2-(*N*-morpholino)ethanesulfonic acid (MES), 1.4 mM $MgCl_2$, 1 mM EDTA, and 2.0 mM guanosine triphosphate (GTP)] for 2 h at 37 °C. The reaction mixture was then centrifuged at 100000*g* in a TLA 120.1 rotor (Beckman) for 1 h at 37 °C. The resulting supernatants and pellets were harvested in Laemmli sample buffer and boiled for 10 min at 100 °C. Samples were absorbed onto nitrocellulose membranes, and the amount of hτ40, β-tubulin, and 3-NT-modified hτ40 in the supernatant and pellet was determined by dot blot using the antibodies Tau-5 (20 ng/mL), 5H1 (0.2 μg/mL), and 3-NT (1 μg/mL), respectively.

RESULTS

$ONOO^-$ Treatment Stabilizes Preformed τ Filaments. Previously, we demonstrated that treatment of full-length human τ (hτ40) monomers with $ONOO^-$ generates heat-stable, SDS-insoluble oligomers (*71*). Further, we established that the increased stability of these oligomers was attributable to covalent 3,3′-DT linkages. Therefore, to examine whether Tyr residues in filamentous hτ40 are accessible to the bulk solvent and, therefore, capable of forming 3,3-DT bonds, hτ40 filaments were assembled in the presence of ArA, isolated via ultracentrifugation, and exposed to a 100-fold molar excess of $ONOO^-$. Samples were then boiled in the presence of SDS and resolved by one-dimensional SDS−PAGE. As shown by Coomassie Brilliant Blue staining, hτ40 filaments are not generated in the absence of ArA inducer (Figure 2, lanes 1 and 4). When incubated in the presence of ArA, however, hτ40 filaments are produced and recovered from the pellet (Figure 2, lanes 2 and 5). Intriguingly, following SDS solubilization at 100 °C, the majority of hτ40 filaments dissociate into their constituent monomers (68 kDa) while only a small percentage remains in multimeric form (≥250 kDa, top and bottom arrows). The SDS solubility of these synthetic hτ40 filaments resembles that of early-stage PHFτ proteins from Alzheimer's brain.

In contrast, hτ40 filaments treated with $ONOO^-$ prior to boiling in SDS detergent display several distinct bands with a reduced mobility by SDS−PAGE (Figure 2, lanes 3 and 6). The lower band at ~69 kDa likely represents nitrated,

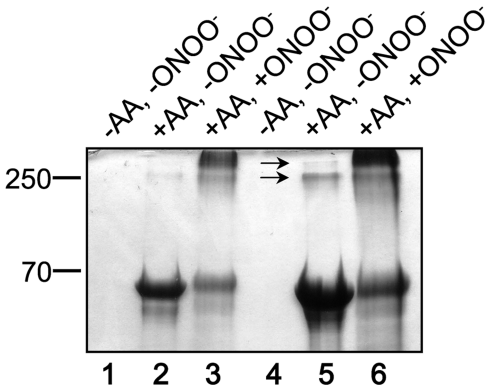

FIGURE 2: Treatment of τ with $ONOO^-$ stabilizes preformed filaments. Monomeric hτ40 proteins were incubated in the presence (lanes 2, 3, 5, and 6) or absence (lanes 1 and 4) of ArA and centrifuged for 1 h at 100000*g* to sediment hτ40 filaments from soluble hτ40 monomers. Pellets were resuspended in nitration buffer, treated with a 100-fold molar excess of active (lanes 3 and 6) or degraded (lanes 2 and 5) $ONOO^-$, boiled in SDS sample buffer, and analyzed by SDS−PAGE with Coomassie Brilliant Blue staining. Twenty-five (lanes 1−3) and fifty (lanes 4−6) micrograms of protein were loaded per well to visualize higher-order aggregate formation. Results are representative of six independent experiments.

monomeric hτ40. This species resolves slightly above the nonmodified monomer because of additional anionic charges that retard gel mobility (*81*). Most strikingly, however, higher-order aggregates appear at molecular masses of >250 kDa (Figure 2, lanes 3 and 6). In fact, much of this high-molecular mass material fails to enter the resolving gel (data not shown). This finding suggests that $ONOO^-$ treatment confers stability upon preformed hτ40 filaments, resulting in their SDS-resistant stabilization and/or aggregation. Moreover, if these higher-order aggregates are, in fact, stabilized via 3,3′-DT bridging, our data suggest that Tyr residues within the hτ40 filament are accessible substrates for $ONOO^-$-mediated modifications.

$ONOO^-$ Treatment Alters Preformed Filament Morphology. We have previously shown that our ArA-induced assembly paradigm accurately models τ polymerization under near-physiological conditions (*82*). In fact, filaments generated from this paradigm morphologically and immunologically resemble authentic τ filaments from AD brain (*83*). To determine the effects of $ONOO^-$ treatment on filament ultrastructure, nonmodified and $ONOO^-$-treated hτ40 filaments (from Figure 2) were visualized by transmission EM. As shown from the micrographs, all nonmodified hτ40 filaments exhibit rodlike, straight filament (SF) morphology with lengths ranging from 0.2 to 1.0 μm (Figure 3A). Numerous small, globular aggregates were also observed (described in ref *83*). It is noteworthy that, following ultracentrifugation, the resuspended hτ40 filaments appear qualitatively similar, in both number and length, to non-resuspended filaments (Figure 3B). Following treatment with $ONOO^-$, however, the SFs manifest an aggregated morphology and appear to be linked with adjacent filaments through interfilament bridges (Figure 3C, arrowheads). As compared to the nonmodified SFs, $ONOO^-$-treated SFs exhibit a paucity of smaller aggregates ($\leq$0.1 μm) (Figure 3C). This latter observation suggests that even the small aggregates may be substrates for $ONOO^-$-mediated cross-linking. Taken together, these data reveal that, following exposure to $ONOO^-$,

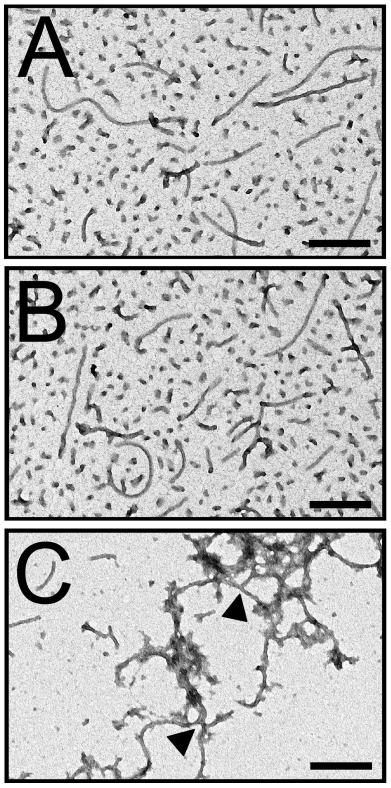

FIGURE 3: Treatment of preformed τ filaments with $ONOO^-$ induces an aggregated morphology. Negative-stain electron micrographs were taken of the nonmodified and $ONOO^-$-treated hτ40 filaments from the experiments in Figure 2. (A) Nonmodified hτ40 filaments prior to resuspension. (B) Nonmodified hτ40 filaments following resuspension. (C) A representative microscopic field of $ONOO^-$-treated hτ40 filaments. The arrowheads illustrate putative cross-linking sites between $ONOO^-$-treated hτ40 filaments. Results are representative of five independent experiments. The calibration bar represents 0.2 μm.

preformed SFs assume an aggregated state that may be attributable to interfilament cross-linking. Furthermore, due to their SDS resistance and reduced mobility by SDS−PAGE (Figure 2), these cross-linked SFs are highly reminiscent of late-stage τ aggregates from autopsy-derived AD brain.

Treatment of SFs with $ONOO^-$ Induces 3,3′-DT Cross-Linking. In an earlier report (*71*), we demonstrated that $ONOO^-$ promotes the oligomerization of hτ40 monomers through formation of covalent 3,3′-DT linkages. This cross-linking event is also responsible for the oligomerization of other neurodegeneration-related proteins, including β-amyloid (*58*) and α-synuclein (*57*, *84*). Therefore, given the robust stability of the $ONOO^-$-treated SFs, we proposed that 3,3′-DT bridging was a likely mechanism behind this aggregation. To test this, hτ40 filaments were assembled in the presence of ArA and treated with a 100-fold molar excess of $ONOO^-$. Size-exclusion chromatography was performed to separate putative 3,3′-DT cross-linked filaments (>250 kDa; Figure 2) from non-cross-linked filaments (250 kDa) and nitrated hτ40 monomers (69 kDa). Each fraction was hydrolyzed into its constituent amino acids and separated by reverse-phase HPLC. As shown from the chromatogram, a peak was observed from the high-molecular mass hydrolysates (>250 kDa) that coeluted with a synthetic 3,3′-DT standard (t_R = 17.6 min) (Figure 4A). This same peak demonstrated the fluorescent excitation and emission signature of 3,3′-DT (λ_{ex} = 283 nm, λ_{em} = 410 nm) (Figure

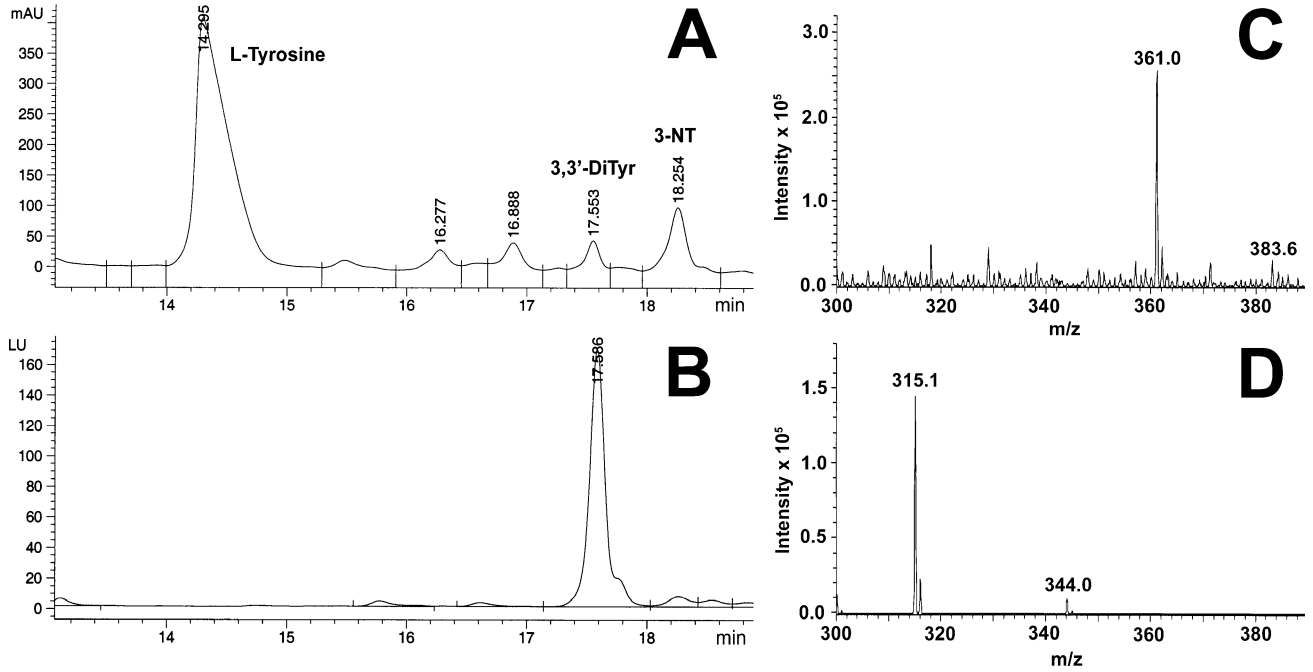

FIGURE 4: Preformed τ filaments are oxidatively cross-linked via 3,3′-DT. Synthetic hτ40 filaments were assembled in the presence of ArA and treated with a 100-fold molar excess of ONOO⁻. High-molecular mass aggregates (>250 kDa) were enriched by size-exclusion chromatography and then hydrolyzed into their constituent amino acids. Reverse-phase HPLC was employed to separate the reaction mixture, and the eluates were monitored by (A) ultraviolet detection at 215 nm and (B) fluorescent detection (λ_{ex} = 283 nm, λ_{em} = 410 nm). (C) ESI-MS analysis of the compound from panel A with a retention time of 17.6 min. (D) Tandem MS/MS scan of the molecular ion $(M + H)^+$ at *m*/*z* 361 from panel C. Results are representative of four independent experiments.

4B). Importantly, a comparable peak was not detected in hydrolysates from the lower-molecular mass fraction (250 kDa) or the nitrated hτ40 monomers (69 kDa) (data not shown). The ESI-MS spectrum of this compound displayed a molecular ion $(M + H)^+$ at *m*/*z* 361, corresponding to the mass of 3,3′-DT (Figure 4C). Collision-induced fragmentation of the precursor ion at *m*/*z* 361 revealed apparent deamination and decarboxylation fragments [$(M + H)^+$ at *m*/*z* 344 and 315, respectively], further confirming the identity of 3,3′-DT (Figure 4D). A peak was also observed by HPLC that coeluted with a purified 3-NT standard (t_R = 18.3 min; Figure 4A) and exhibited the mass [$(M + H)^+$ at *m*/*z* 227] and fragmentation properties of 3-NT (data not shown). Collectively, these findings suggest that the higher-order aggregates generated from ONOO⁻ treatment of preformed SFs are stabilized via 3,3′-DT bonds.

Nitration of Synthetic τ Filaments Occurs with Site Specificity. Protein nitration occurs with biological selectivity and can profoundly alter protein folding and function (*42*−*45*, *52*−*56*). Previously, we demonstrated that ONOO⁻-mediated nitration of hτ40 monomers occurs with site specificity (Tyr18 and Tyr29 ≫ Tyr197 and Tyr394) (*69*, *71*). The cumulative effect of this event was to significantly inhibit hτ40 polymerization in vitro (*71*). Therefore, because filamentous hτ40 is conformationally distinct from monomeric hτ40 (*28*), we assayed for site-selective nitration in hτ40 filaments. Accordingly, wild-type and mutant hτ40 proteins were polymerized in the presence of ArA and then treated with a 100-fold molar excess of ONOO⁻. It should be noted that the equilibrium polymer mass is equivalent for each of these mutant proteins, including the quintuple hτ40 mutant lacking all Tyr residues (termed ^{5x}Y→F) (*69*). ONOO⁻-treated wild-type and mutant hτ40 filaments were then passed over centrifugal filter columns (100 kDa molecular mass cutoff) to remove residual hτ40 monomers. Western blot analysis with a Tau-5 antibody confirmed that, following filtration, monomeric hτ40 was absent from the samples (data not shown). Total hτ40 and 3-NT-modified hτ40 were detected by dot blot using the Tau-5 and 3-NT antibodies, respectively.

Following ONOO⁻ treatment, hτ40 filaments were preferentially nitrated at the amino terminus (Tyr18 and Tyr29), as opposed to the proline-rich (Tyr197), MT-binding repeat (Tyr310), and carboxy-terminal (Tyr394) regions (Figure 5A). The relative 3-NT immunoreactivity of each mutant sample was then normalized to Tau-5 and represented as a percentage of wild-type filament 3-NT reactivity. As shown from the histograms, mutant filaments containing a single Tyr at position Tyr18 (^{18}Y) and Tyr29 (^{29}Y) exhibit near-identical levels of reactivity toward the 3-NT antibody (94 ± 7.4 A_{450} units and 94 ± 7.2 A_{450} units, respectively) (Figure 5B). In fact, the 3-NT immunoreactivity of the nitrated ^{18}Y and ^{29}Y mutant filaments does not significantly differ from that of the nitrated wild-type filaments. This finding suggests that, in wild-type filaments, residues Tyr18 and Tyr29 are the primary substrates for ONOO⁻-mediated nitration and, consequently, are nitrated to equivalent degrees. However, in mutant filaments harboring a single Tyr residue at position Tyr18 or Tyr29 (mutant ^{18}Y or ^{29}Y, respectively), nitration at each site occurs with a two-fold greater efficiency as compared to wild-type filaments due to less competition between the amino-terminal Tyr substrates. While nitration does occur in the ^{197}Y and ^{394}Y mutant filaments (9.0 ± 2.5 A_{450} units and 8.6 ± 2.6 A_{450} units, respectively), this 3-NT reactivity is significantly lower than that of the nitrated ^{18}Y and ^{29}Y mutant filaments (Figure 5B; $p < 0.0005$ in all comparisons). As predicted from studies in the hτ40 monomer (*71*), nitration of the ^{310}Y mutant filaments is negligible.

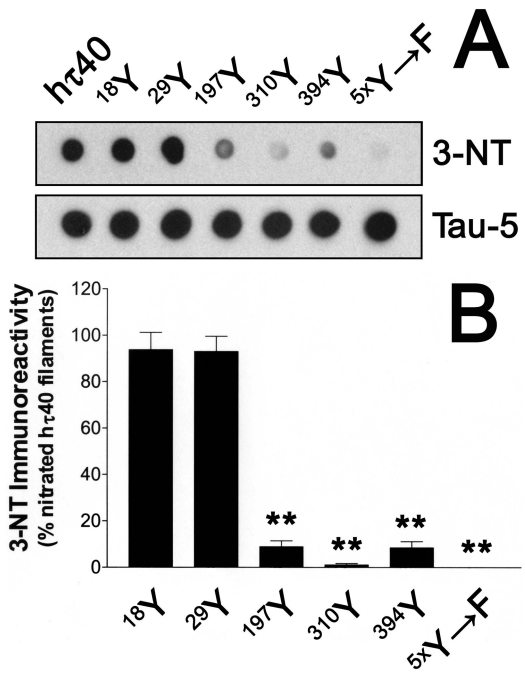

FIGURE 5: Nitration occurs with site specificity on preformed τ filaments. Nitrated wild-type and nitrated mutant hτ40 filaments were enriched by centrifugal filtration and adsorbed onto nitrocellulose membranes for dot blot analyses. (A) Nitrocellulose membranes were probed with a Tau-5 or 3-NT antibody to assay for total hτ40 protein or 3-NT-modified hτ40 protein, respectively. (B) The 3-NT signal from each filamentous mutant in panel A was normalized to Tau-5 and represented as a percentage of wild-type filament 3-NT reactivity. Results are from five independent experiments and are plotted as the mean ± SEM. The Student's two-tailed *t* test was used to compare mean 3-NT immunoreactivities between nitrated wild-type and nitrated mutant hτ40 filaments (**$p < 0.0005$).

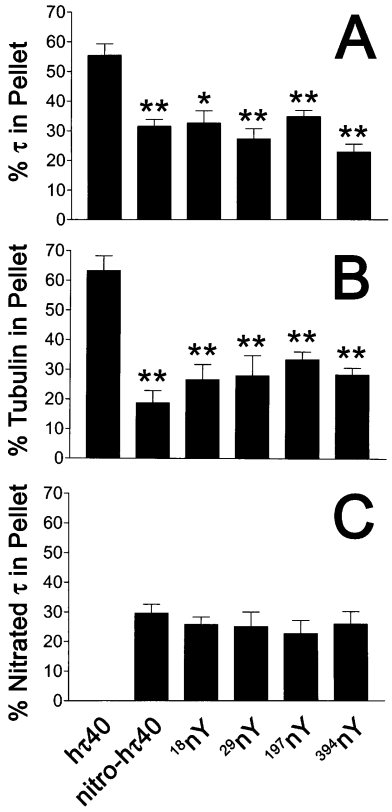

FIGURE 6: Site-specific nitration attenuates MT binding and stabilization. Phosphocellulose-purified tubulin was copolymerized in the presence of wild-type, nitrated wild-type, or nitrated mutant hτ40 proteins until steady state was achieved. High-speed ultracentrifugation was performed to separate MT-bound (pellet) from MT-unbound (supernatant) hτ40, and the percentage of hτ40 in the pellet was quantified using dot blot analyses. Nitrocellulose membranes were probed for (A) total hτ40, (B) β-tubulin, and (C) 3-NT-modified hτ40 using the Tau-5, 5H1, and 3-NT antibodies, respectively. Results are from six independent experiments and are plotted as the mean ± SEM. The Student's two-tailed *t* test was used to compare mean percentages between wild-type nitrated hτ40 proteins (*$p < 0.05$; **$p < 0.005$).

Collectively, these findings reveal that $ONOO^-$-mediated nitration of hτ40 filaments occurs in a hierarchical pattern similar to that seen in the hτ40 monomer.

Site-Specific τ Nitration Destabilizes MTs. Since several posttranslational modifications alter the ability of τ to promote tubulin assembly (*68*), we examined whether mutant τ proteins singly nitrated at residues Tyr18 (termed ^{18}nY), Tyr29 (^{29}nY), Tyr197 (^{197}nY), and Tyr394 (^{394}nY) influence MT stability. Although we have described these mutants previously (*69*), we did not determine the molar percentage of 3-NT in each sample. Therefore, to quantify the percentage of nitrated versus nonnitrated hτ40 in each preparation, amino acid analysis (AAA) was performed. However, due to the chemical instability of the 3-NT moiety, the molar percentage of Tyr consumed following $ONOO^-$ treatment was used as a surrogate measure of nitration: ^{18}nY (95% nitrated), ^{29}nY (100% nitrated), ^{197}nY (45% nitrated), and ^{394}nY (54% nitrated). The nitration levels calculated by this method closely approximate the 3-NT immunoreactivities previously reported for each nitrated mutant (*69*). Importantly, by both AAA and ESI-MS, we found no evidence of oxidative derivatization of other susceptible residues, suggesting that Tyr nitration is the primary modification. It should also be noted that a ^{310}nY mutant was not included in these analyses because we previously showed that $ONOO^-$-mediated nitration occurs infrequently at this position in vitro (*71*).

In each experiment, tubulin dimers (10 μM) were copolymerized with wild-type, nitrated wild-type, or nitrated mutant hτ40 proteins (2 μM) until steady state was achieved. Cosedimentation of the τ-tubulin reaction mixture was then performed using high-speed centrifugation, and the percentage of total hτ40, β-tubulin, and 3-NT-modified hτ40 in the pellet was determined by immunoblot analysis using the Tau-5, 5H1, and 3-NT antibodies, respectively.

Our rationale for using this copolymerization strategy was three-fold. First, the concentrations of τ and tubulin used in the assay closely approximate those found in human brain (*22*, *85*). Second, analogous to the in vivo scenario, our cosedimentation assay takes into consideration the presence of τ *during* tubulin assembly. Finally, and perhaps most importantly, the molar ratio of τ to tubulin used in the assay (1:5) lies within the saturable range of τ−tubulin binding kinetics (*86*).

As evidenced from the histograms, slightly more than half (55 ± 3.9%) of the total wild-type hτ40 was recovered from the pellet, or MT-bound fraction, following centrifugation (Figure 6A). This percentage of MT-bound τ closely approximates the value obtained in an earlier report using a similar experimental approach (*86*). Intriguingly, all 3-NT-modified hτ40 proteins, both wild-type and mutant, are significantly reduced in the MT-bound fraction (~22−34%

of total hτ40 protein) as compared to nonmodified hτ40 ($p < 0.05$ in all comparisons). In a control experiment in which tubulin was omitted from the copolymerization reaction, no hτ40 was recovered from the pellet (data not shown). Moreover, to rule out the possibility that Tyr → Phe mutagenesis of hτ40 influences MT binding and stabilization, tubulin dimers were copolymerized in the presence of nonmodified hτ40 mutants (i.e. ^{18}Y, ^{29}Y, ^{197}Y, ^{394}Y, and ^{5x}Y→F). These nonmodified mutants did not differ significantly from wild-type hτ40 in their ability to promote tubulin assembly (data not shown).

To determine whether the diminution of MT-bound hτ40 was attributable to a reduced capacity of the nitrated hτ40 proteins to stabilize MTs, the percentage of tubulin in the pellet was also measured. Significantly, the percentage of tubulin recovered from the pellet following copolymerization with wild-type hτ40 (61 ± 5.5%) was greater than the percentage recovered after coincubation with nitrated wild-type and nitrated mutant hτ40 proteins (∼18−33%; $p <$ 0.005 in all comparisons) (Figure 6B). Moreover, when tubulin was co-assembled with nitrated wild-type or nitrated mutant hτ40, the majority of 3-NT-modified proteins (∼70−77%) were dissociated from the MT lattice (Figure 6C). Taken together, these data show that site-specific nitration at Tyr18, Tyr29, Tyr197, and Tyr394 modulates the ability of monomeric hτ40 to promote tubulin assembly. These findings suggest that, in vivo, τ nitration may induce a pathological loss of function due to deficient MT binding and stabilization.

Pseudophosphorylation of τ Does Not Affect MT Stability. Posttranslational phosphorylation is an event known to influence τ−MT interactions (*68*). Therefore, to determine whether Tyr phosphorylation also attenuates the ability of τ to promote tubulin polymerization, we performed cosedimentation assays using hτ40 mutants pseudophosphorylated at each Tyr residue. As demonstrated by dot blot analysis, hτ40 mutants that mimic phosphorylation at residues Tyr18 ($^{Y}18^{E}$), Tyr29 ($^{Y}29^{E}$), Tyr197 ($^{Y}197^{E}$), Tyr310 ($^{Y}310^{E}$), and Tyr394 ($^{Y}394^{E}$) do not influence the distribution of MT-bound versus MT-unbound hτ40 relative to the wild-type control (Figure 7A). To exclude the possibility that the Tyr → Glu hτ40 mutants differentially promote tubulin assembly, we assayed the relative amounts of tubulin in the supernatant and pellet. Interestingly, each pseudophosphorylated hτ40 mutant was able to bind and stabilize MTs to an extent similar to that of the wild-type protein (Figure 7B). Our findings closely agree with a previous report showing that Fyn-mediated Tyr18 phosphorylation does not influence the binding of τ to taxol-stabilized MTs (*87*). Collectively, these data reveal that the biochemical nature of the 3-NT moiety specifically disrupts τ−MT interactions.

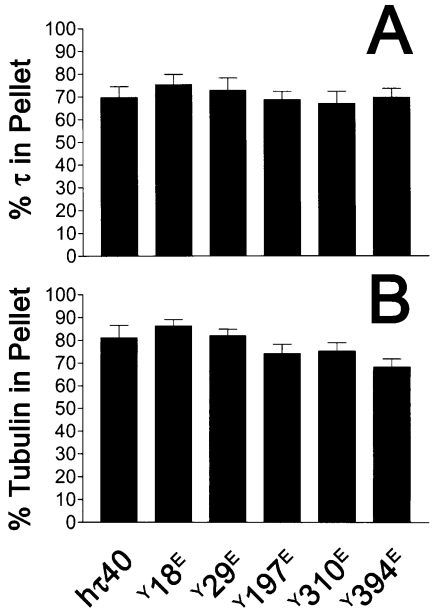

FIGURE 7: Pseudophosphorylation of τ does not influence tubulin assembly. Phosphocellulose-purified tubulin was copolymerized in the presence of hτ40 mutants pseudophosphorylated (Tyr → Glu) at each Tyr residue. After steady state was achieved, high-speed ultracentrifugation was performed to separate MT-bound (pellet) from MT-unbound (supernatant) hτ40. The percentage of hτ40 in the pellet was then quantified using dot blot analyses. Nitrocellulose membranes were probed for (A) total hτ40 and (B) β-tubulin using the Tau-5 and 5H1 antibodies, respectively. Results are from five independent experiments and are plotted as the mean ± SEM. The Student's two-tailed *t* test was used to compare mean percentages between wild-type and mutant hτ40 proteins.

DISCUSSION

Evidence from recent years has ushered in a new perspective in posttranslational τ biology. Apart from the canonical belief that Ser and/or Thr phosphorylation precipitates τ misfolding, deposition, and displacement from MTs, numerous reports reveal that other posttranslational events assume a critical role in τ dysfunction. Specifically, proteolysis (*24*), conformational changes (*25*−*27*), glycation (*88*), glycosylation (*89*), ubiquitination (*90*−*92*), transglutamination (*93*), and polyamination (*94*) have all been implicated in the series of events preceding fibrillar τ pathology. Additionally, nitration, an event formerly relegated to the role of a nonspecific, end-stage modification of little biological significance, occurs on the τ protein in post-mortem AD brain (*95*). In fact, we have previously demonstrated that τ is a substrate for ONOO⁻-mediated nitrative and oxidative modification (*71*). While the former event attenuates τ polymerization in vitro, the latter induces the SDS-resistant oligomerization of τ monomers through the formation of covalent 3,3′-DT linkages (*71*). More recently, we showed that site-specific nitration differentially influences the rate and/or extent of τ assembly in vitro, significantly altering both the filamentous mass and critical concentration (*69*). These findings strongly support the role of nitration as a biologically selective event that can profoundly alter protein function (*52*).

As an extension of our previous work, this study was designed to examine the effects of ONOO⁻-mediated modifications on two aspects of τ pathophysiology: (1) the stability of preformed τ filaments and (2) the capacity of monomeric τ to promote tubulin polymerization. Here, we show that treatment of τ with ONOO⁻ cross-links preformed filaments and attenuates the binding of monomeric τ to MTs though distinct oxidative and nitrative mechanisms, respectively. While 3,3′-DT linkages are the likely mechanism through which ONOO⁻ induces τ filament aggregation, nitrative modifications inhibit the ability of τ monomers to bind and stabilize MTs. Importantly, the MT binding deficits exhibited by τ monomers selectively nitrated at residues Tyr18, Tyr29, Tyr197, and Tyr394 cannot be replicated by pseudophosphorylation at these same residues. This latter

finding suggests that τ nitration specifically disrupts τ−MT interactions. Collectively, our data lend mechanistic insights into the process by which nitrative and oxidative modifications may influence τ function in AD pathogenesis.

Implications for ONOO⁻-Mediated PHFτ Cross-Linking in Vivo. PHFτ derived from postmortem AD brain exhibits striking biochemical characteristics, including stringent insolubility and resistance to proteolytic degradation. Intriguingly, however, the solubility of PHFτ in SDS-based detergents changes during the course of PHF maturation. For example, early-stage PHFτ [also termed A68 (*96*)] demonstrates SDS solubility and is comprised of hyperphosphorylated, full-length τ (*96*, *97*). These early-stage PHFτ proteins exhibit a markedly reduced mobility by SDS−PAGE and are incapable of promoting tubulin assembly (*98*−*100*). During late-stage maturation, PHFτ consists mainly of the carboxy third of the τ molecule and demonstrates SDS insolubility (*101*, *102*). Clearly, during the transition from early- to late-stage PHFτ, a stabilizing event occurs that imparts structural stability to the PHF proteins.

In the present study, we show that ArA-induced τ filaments, which morphologically and immunologically resemble AD-derived filaments (*83*), manifest many of the biochemical properties of early-stage PHFτ proteins. For instance, these synthetic filaments readily dissociate into their constituent monomers following boiling in SDS detergents (Figure 2). We further demonstrate that treatment with ONOO⁻ not only stabilizes preexisting τ filaments but also induces their SDS-resistant oligomerization. Therefore, one potential in vivo correlate to our findings is that ONOO⁻-mediated 3,3′-DT bridging stabilizes early-stage PHFτ proteins and renders them SDS-resistant. Following this irreversible cross-linking event, the SDS-soluble, early-stage PHFτ proteins are converted into SDS-insoluble, late-stage PHFτ proteins. This highly stable PHFτ species may then exert a direct toxic effect on the neuron and lead to τ-induced neurodegeneration.

Several reports have shown that proteolytic processing at the amino terminus occurs during late-stage PHFτ maturation (*27*, *103*). Given that ONOO⁻-mediated 3,3′-DT cross-linking of τ occurs predominantly at the amino terminus (*71*), an intriguing possibility is that amino-terminal truncation prevents the formation of 3,3′-DT linkages. Therefore, in early-stage tangles containing τ with an intact amino terminus (i.e. PHFτ), 3,3′-DT may be a stabilizing event that maintains aggregation. In contrast, τ filaments assembled from carboxy-terminal fragments may be less toxic than other τ species due to a lack of 3,3′-DT stabilization. Our data, however, cannot exclude the possibility that residues Tyr197, Tyr310, and Tyr394 also participate in 3,3′-DT formation in vivo. Moreover, other covalent cross-linking events, such as transglutamination (*93*) and/or glycation (*104*), may also stabilize filaments at different stages in the disease process, depending upon the cleavage state and/or conformation of τ.

It is worth noting that the level of 3,3′-DT detected in the ONOO⁻-treated τ filaments (Figure 4) was significantly lower than the amount of 3,3′-DT recovered from the ONOO⁻-treated τ monomers (compare with data from ref *71*). This observation suggests that, in the filamentous form, τ subunits may be aligned in a manner that diminishes ONOO⁻ accessibility to the Tyr substrate. Further, although ONOO⁻-mediated interfilament cross-linking appears to be less efficient than cross-linking of the natively unfolded τ monomer, it nonetheless generates a considerable mass of aggregated filaments (Figure 2, top arrow). Accordingly, because fewer 3,3′-DT bonds are required to link filaments in vitro as compared to τ monomers, levels of ONOO⁻-induced cross-linking may be relatively low in vivo and still exert profound effects on filament solubility.

Detection of 3,3′-DT-Linked τ in AD Brain. Clearly, detection of 3,3′-DT-linked τ in human AD brain is an important step toward validating our in vitro findings. However, while characterization of 3,3′-DT is feasible in vitro due to the purity and abundance of recombinant proteins (*57*, *71*), similar in vivo analyses are frustrated by sample contamination and yield. For example, we have recently purified PHFτ from AD brain homogenates and subjected these samples to LC−MS/MS analyses. Unfortunately, our efforts to detect 3,3′-DT-linked PHFτ were unsuccessful for two primary reasons. First, the recovery of PHFτ from AD brain is low (<1 μg of PHFτ/g of gray matter) (*105*). Accordingly, if 1−5% of the total PHFτ is 3,3′-DT-linked, then a 20 g preparation would, at best, yield ∼1 μg of 3,3′-DT-linked PHFτ, or ∼10 pmol of the hydrolyzed 3,3′-DT product. Subsequent enrichment and purification steps would necessarily reduce this yield. While 10 pmol of 3,3′-DT lies within the theoretical limits of detection for most LC/ESI-MS instruments, we observed other peaks that masked the molecular ion for 3,3′-DT. Therefore, despite using purified PHFτ and highly sensitive mass spectrometric analyses, reaction products that coelute with 3,3′-DT-linked PHFτ confounded biochemical analyses. To our knowledge, there have been few, if any, reports on *specific* 3,3′-DT-linked proteins recovered from human tissues. While levels of 3,3′-DT have been shown to be elevated in AD brain using LC with electrochemical detection (*106*), this study reported *free* 3,3′-DT following proteolysis.

In addition to our biochemical efforts, we have attempted to colocalize τ and 3,3′-DT immunohistochemically using antibodies that recognize 3,3′-DT in a manner that is independent of protein context (*107*). The results of these experiments revealed no specific 3,3′-DT staining in any of the control or severe AD cases (Braak stage V−VI) examined. It should also be noted that the immunogen used to generate these 3,3′-DT antibodies was structurally similar, but not identical, to 3,3′-DT. In our hands, these antibodies detected enzymatically produced 3,3′-DT in solid-phase assays but did not detect ONOO⁻-induced 3,3′-DT in the same solid-phase assays (data not shown). This observation questions the usefulness of these reagents as an accurate means of detecting 3,3′-DT and underscores the need for *protein-specific* 3,3′-DT antibodies.

Nitration of τ Modulates MT Binding and Stabilization. PHFτ proteins purified from autopsy-derived AD brain exhibit a reduced ability to promote tubulin assembly, a finding attributed to their abnormal phosphorylation (*100*). Therefore, to examine whether site-specific τ nitration recapitulates this effect, copolymerization assays were performed using τ mutants singly nitrated at residues Tyr18, Tyr29, Tyr197, and Tyr394. Our data demonstrate that NO_2 occupancy at any of these Tyr residues markedly inhibits tubulin polymerization relative to the effect of nonmodified τ. Further, this inhibition of tubulin assembly is specific to

the 3-NT modification, as τ mutants pseudophosphorylated at each Tyr residue exhibit the assembly-promoting ability of wild-type τ.

Initially, we were surprised that select nitration of the amino terminus (i.e. Tyr18 and Tyr29) and proline-rich regions (i.e. Tyr197) of τ significantly attenuates MT binding. This was largely because these regions lie upstream of the MT-binding domains. However, the amino terminus and proline-rich regions of τ are believed to impart the flexibility and molecular spacing needed for conformational changes to occur (*64*). In fact, it has been proposed that while the natively unfolded τ monomer undergoes a wide range of conformers in solution, it becomes locked in a specific conformation once engaged at the MT surface (*108*). This notion is supported by kinetic analyses showing that the $\tau-$MT interaction is a two-step process that likely involves a conformational change in τ prior to MT binding (*109*). Therefore, it is entirely possible that nitration of the amino terminus and proline-rich regions prevents specific τ conformations that are necessary for $\tau-$MT interactions.

Perhaps the most unexpected finding was that, despite having markedly *different* levels of nitration, each nitrated τ mutant inhibits MT binding to a *similar* extent. One explanation for this effect may be found within the "jaws" model of $\tau-$MT binding (*110*, *111*). In this paradigm, the regions immediately flanking the MT-binding repeats, termed the "targeting" domains, are responsible for anchoring τ onto the MT. Once τ engages the MT surface, the MT-binding repeats then catalytically promote MT assembly. Evidence showing that the targeting domains of τ bind with much greater avidity to the MT surface than the MT-binding domains themselves ($K_d = 1$ and 10^2-10^3 μM, respectively) supports this contention (*112*, *113*). Thus, given the location of Tyr197 and Tyr394 within these targeting regions, it is feasible that nitration at these sites would inhibit MT binding with greater efficacy than nitration at Tyr18 and Tyr29, even though these residues are nitrated to a lesser extent.

In an earlier report, we demonstrated that the Alz-50 antibody binds filaments assembled from nitrated τ monomers with higher avidity than wild-type filaments, even in instances where the overall filamentous mass is reduced (*69*). Those data also reveal that the Alz-50 epitope may be achieved in the absence of bona fide τ filaments. Therefore, in addition to destabilizing the MT network, site-selective τ nitration appears to stabilize the pathological Alz-50 conformation. A logical inference from these findings would be that the Alz-50 epitope is conformationally incompatible with MT binding. This concept is reinforced by multiple lines of evidence showing that Alz-50$^+$ PHFτ proteins are unable to promote tubulin assembly (*114*−*116*).

If τ nitration stabilizes the Alz-50 conformation and, consequently, destabilizes MTs in vivo, this event may help to integrate the pathological gain- and loss-of-function mechanisms for τ-induced neurodegeneration. Specifically, during AD pathogenesis, τ undergoes abnormal modifications (i.e. hyperphosphorylation) that promote the Alz-50 conformation. Assumption of the Alz-50 epitope may then reduce MT binding [likely by sequestering the MTBR region (*28*)] and increase the intracellular pool of free τ available for polymerization. After overcoming a critical concentration threshold of $\sim$0.5 μM (*69*), filaments can self-assemble via mass action and perhaps exert a direct, toxic effect on the neuron. Stabilization and/or aggregation of preformed τ filaments via 3,3′-DT linkages may also contribute to this neurotoxicity. Concomitantly, the resulting loss of MT dynamics would indirectly lead to neuronal death (*117*).

In contrast, while nitration of τ monomers promotes the Alz-50 epitope and reduces MT stability, this event renders τ assembly-incompetent due to a significantly increased critical concentration (*69*). Moreover, because 3-NT addition destabilizes the aromatic Tyr ring toward further oxidative modifications (*57*), the likelihood of 3,3′-DT cross-linking would be diminished. Therefore, following 3-NT modification of the τ protein, the potential for a toxic gain-of-function effect may be markedly reduced. The finding that hippocampal neurons expressing nitric oxide synthase, an enzyme promoting ONOO$^-$ production, are not susceptible to AD-associated neurodegeneration (*118*) supports the role of τ nitration as a neuroprotective event.

It is important to note that the effects of ONOO$^-$-mediated τ nitration on MT binding were recently examined by another group (*119*). However, several critical differences exist between the earlier report and our study. First, the previous study did not separate the ONOO$^-$-induced oligomers from the nitrated τ monomers prior to the MT binding assays. Thus, the potentially confounding effects of the 3,3′-DT-linked oligomers were not taken into consideration. Second, because the study focused on nitration of the wild-type three-repeat (hτ39) τ protein, the effects of 3-NT modification at *specific* Tyr residues were not addressed. Finally, the MT binding assays in the previous study employed taxol-stabilized MTs. While this technique is commonly utilized to measure substrate−MT interactions, it inaccurately models the in vivo scenario where tubulin is assembled in the *presence* of τ.

Conclusions. In summary, ONOO$^-$-mediated modifications exert dichotomous and antagonistic effects on τ function in vitro. On one hand, oxidative 3,3′-DT cross-linking promotes the SDS-resistant oligomerization of τ monomers (*71*) and also aggregates preformed τ filaments. On the other hand, ONOO$^-$-mediated nitration alters τ polymerization kinetics, filament morphology, equilibrium polymer mass, critical concentration, and the ability of monomeric τ to support tubulin assembly. The cumulative effect of these modifications on τ function in vivo may be attributable to the balance of ONOO$^-$-mediated oxidation and nitration, and the conditions that favor these reactions. Taken together, our findings speak to the multifaceted role of oxidative and nitrative τ modifications in vitro and provide critical insights into how these events may influence τ function in vivo.

ACKNOWLEDGMENT

We acknowledge Dr. Sarah Rice (Northwestern University) for invaluable advice and assistance with the tubulin preparation and cosedimentation assays. We also thank Phillip C. Lesh and Ron McKernan for inspiration and guidance. LC−MS/MS and HPLC experiments were performed at the Analytical Services Laboratory and Keck Biophysics Facility of Northwestern University, respectively. Transmission EM was conducted at the Cell Imaging Facility of Northwestern University. Amino acid analyses were carried out at the Molecular Structure Facility at the University of California Davis.

REFERENCES

1. Morris, J. C., Heyman, A., Mohs, R. C., Hughes, J. P., van Belle, G., Fillenbaum, G., Mellits, E. D., and Clark, C. (1989) The Consortium to Establish a Registry for Alzheimer's Disease (CERAD). Part I. Clinical and neuropsychological assessment of Alzheimer's disease, *Neurology 39*, 1159−65.
2. Brion, J. P., Hanger, D. P., Couck, A. M., and Anderton, B. H. (1991) A68 proteins in Alzheimer's disease are composed of several tau isoforms in a phosphorylated state which affects their electrophoretic mobilities, *Biochem. J. 279* (Part 3), 831−6.
3. Kidd, M. (1963) Paired helical filaments in electron microscopy of Alzheimer's disease, *Nature 197*, 192−3.
4. Kosik, K. S., Joachim, C. L., and Selkoe, D. J. (1986) Microtubule-associated protein tau (tau) is a major antigenic component of paired helical filaments in Alzheimer disease, *Proc. Natl. Acad. Sci. U.S.A. 83*, 4044−8.
5. Wischik, C. M., Novak, M., Edwards, P. C., Klug, A., Tichelaar, W., and Crowther, R. A. (1988) Structural characterization of the core of the paired helical filament of Alzheimer disease, *Proc. Natl. Acad. Sci. U.S.A. 85*, 4884−8.
6. Wischik, C. M., Novak, M., Thogersen, H. C., Edwards, P. C., Runswick, M. J., Jakes, R., Walker, J. E., Milstein, C., Roth, M., and Klug, A. (1988) Isolation of a fragment of tau derived from the core of the paired helical filament of Alzheimer disease, *Proc. Natl. Acad. Sci. U.S.A. 85*, 4506−10.
7. Glenner, G. G., and Wong, C. W. (1984) Alzheimer's disease: Initial report of the purification and characterization of a novel cerebrovascular amyloid protein, *Biochem. Biophys. Res. Commun. 120*, 885−90.
8. Arriagada, P. V., Growdon, J. H., Hedley-Whyte, E. T., and Hyman, B. T. (1992) Neurofibrillary tangles but not senile plaques parallel duration and severity of Alzheimer's disease, *Neurology 42*, 631−9.
9. Foster, N. L., Wilhelmsen, K., Sima, A. A., Jones, M. Z., D'Amato, C. J., and Gilman, S. (1997) Frontotemporal dementia and parkinsonism linked to chromosome 17: A consensus conference. Conference Participants, *Ann. Neurol. 41*, 706−15.
10. Hutton, M., Lendon, C. L., Rizzu, P., Baker, M., Froelich, S., Houlden, H., Pickering-Brown, S., Chakraverty, S., Isaacs, A., Grover, A., Hackett, J., Adamson, J., Lincoln, S., Dickson, D., Davies, P., Petersen, R. C., Stevens, M., de Graaff, E., Wauters, E., van Baren, J., Hillebrand, M., Joosse, M., Kwon, J. M., Nowotny, P., Heutink, P., et al. (1998) Association of missense and 5′-splice-site mutations in tau with the inherited dementia FTDP-17, *Nature 393*, 702−5.
11. Poorkaj, P., Bird, T. D., Wijsman, E., Nemens, E., Garruto, R. M., Anderson, L., Andreadis, A., Wiederholt, W. C., Raskind, M., and Schellenberg, G. D. (1998) Tau is a candidate gene for chromosome 17 frontotemporal dementia, *Ann. Neurol. 43*, 815−25.
12. Mucke, L., Masliah, E., Yu, G. Q., Mallory, M., Rockenstein, E. M., Tatsuno, G., Hu, K., Kholodenko, D., Johnson-Wood, K., and McConlogue, L. (2000) High-level neuronal expression of Aβ1−42 in wild-type human amyloid protein precursor transgenic mice: Synaptotoxicity without plaque formation, *J. Neurosci. 20*, 4050−8.
13. Hsiao, K., Chapman, P., Nilsen, S., Eckman, C., Harigaya, Y., Younkin, S., Yang, F., and Cole, G. (1996) Correlative memory deficits, Aβ elevation, and amyloid plaques in transgenic mice, *Science 274*, 99−102.
14. Chishti, M. A., Yang, D. S., Janus, C., Phinney, A. L., Horne, P., Pearson, J., Strome, R., Zuker, N., Loukides, J., French, J., Turner, S., Lozza, G., Grilli, M., Kunicki, S., Morissette, C., Paquette, J., Gervais, F., Bergeron, C., Fraser, P. E., Carlson, G. A., George-Hyslop, P. S., and Westaway, D. (2001) Early-onset amyloid deposition and cognitive deficits in transgenic mice expressing a double mutant form of amyloid precursor protein 695, *J. Biol. Chem. 276*, 21562−70.
15. Rapoport, M., Dawson, H. N., Binder, L. I., Vitek, M. P., and Ferreira, A. (2002) Tau is essential to β-amyloid-induced neurotoxicity, *Proc. Natl. Acad. Sci. U.S.A. 99*, 6364−9.
16. Schweers, O., Schonbrunn-Hanebeck, E., Marx, A., and Mandelkow, E. (1994) Structural studies of tau protein and Alzheimer paired helical filaments show no evidence for β-structure, *J. Biol. Chem. 269*, 24290−7.
17. Cleveland, D. W., Hwo, S. Y., and Kirschner, M. W. (1977) Purification of tau, a microtubule-associated protein that induces assembly of microtubules from purified tubulin, *J. Mol. Biol. 116*, 207−25.
18. von Bergen, M., Barghorn, S., Li, L., Marx, A., Biernat, J., Mandelkow, E. M., and Mandelkow, E. (2001) Mutations of tau protein in frontotemporal dementia promote aggregation of paired helical filaments by enhancing local β-structure, *J. Biol. Chem. 276*, 48165−74.
19. von Bergen, M., Friedhoff, P., Biernat, J., Heberle, J., Mandelkow, E. M., and Mandelkow, E. (2000) Assembly of tau protein into Alzheimer paired helical filaments depends on a local sequence motif ((306)VQIVYK(311)) forming β structure, *Proc. Natl. Acad. Sci. U.S.A. 97*, 5129−34.
20. Giannetti, A. M., Lindwall, G., Chau, M. F., Radeke, M. J., Feinstein, S. C., and Kohlstaedt, L. A. (2000) Fibers of tau fragments, but not full length tau, exhibit a cross β-structure: Implications for the formation of paired helical filaments, *Protein Sci. 9*, 2427−35.
21. Grundke-Iqbal, I., Iqbal, K., Tung, Y. C., Quinlan, M., Wisniewski, H. M., and Binder, L. I. (1986) Abnormal phosphorylation of the microtubule-associated protein tau (tau) in Alzheimer cytoskeletal pathology, *Proc. Natl. Acad. Sci. U.S.A. 83*, 4913−7.
22. Alonso, A. C., Grundke-Iqbal, I., and Iqbal, K. (1996) Alzheimer's disease hyperphosphorylated tau sequesters normal tau into tangles of filaments and disassembles microtubules, *Nat. Med. 2*, 783−7.
23. Wood, J. G., Mirra, S. S., Pollock, N. J., and Binder, L. I. (1986) Neurofibrillary tangles of Alzheimer disease share antigenic determinants with the axonal microtubule-associated protein tau (tau), *Proc. Natl. Acad. Sci. U.S.A. 83*, 4040−3.
24. Gamblin, T. C., Chen, F., Zambrano, A., Abraha, A., Lagalwar, S., Guillozet, A. L., Lu, M., Fu, Y., Garcia-Sierra, F., LaPointe, N., Miller, R., Berry, R. W., Binder, L. I., and Cryns, V. L. (2003) Caspase cleavage of tau: Linking amyloid and neurofibrillary tangles in Alzheimer's disease, *Proc. Natl. Acad. Sci. U.S.A. 100*, 10032−7.
25. Ghoshal, N., Garcia-Sierra, F., Fu, Y., Beckett, L. A., Mufson, E. J., Kuret, J., Berry, R. W., and Binder, L. I. (2001) Tau-66: Evidence for a novel tau conformation in Alzheimer's disease, *J. Neurochem. 77*, 1372−85.
26. Ghoshal, N., Garcia-Sierra, F., Wuu, J., Leurgans, S., Bennett, D. A., Berry, R. W., and Binder, L. I. (2002) Tau conformational changes correspond to impairments of episodic memory in mild cognitive impairment and Alzheimer's disease, *Exp. Neurol. 177*, 475−93.
27. Garcia-Sierra, F., Ghoshal, N., Quinn, B., Berry, R. W., and Binder, L. I. (2003) Conformational changes and truncation of tau protein during tangle evolution in Alzheimer's disease, *J. Alzheimer's Dis. 5*, 65−77.
28. Carmel, G., Mager, E. M., Binder, L. I., and Kuret, J. (1996) The structural basis of monoclonal antibody Alz50's selectivity for Alzheimer's disease pathology, *J. Biol. Chem. 271*, 32789−95.
29. Hyman, B. T., Van Hoesen, G. W., Wolozin, B. L., Davies, P., Kromer, L. J., and Damasio, A. R. (1988) Alz-50 antibody recognizes Alzheimer-related neuronal changes, *Ann. Neurol. 23*, 371−9.
30. Novak, M., Jakes, R., Edwards, P. C., Milstein, C., and Wischik, C. M. (1991) Difference between the tau protein of Alzheimer paired helical filament core and normal tau revealed by epitope analysis of monoclonal antibodies 423 and 7.51, *Proc. Natl. Acad. Sci. U.S.A. 88*, 5837−41.
31. Bondareff, W., Wischik, C. M., Novak, M., Amos, W. B., Klug, A., and Roth, M. (1990) Molecular analysis of neurofibrillary degeneration in Alzheimer's disease. An immunohistochemical study, *Am. J. Pathol. 137*, 711−23.
32. Bondareff, W., Harrington, C., Wischik, C. M., Hauser, D. L., and Roth, M. (1994) Immunohistochemical staging of neurofibrillary degeneration in Alzheimer's disease, *J. Neuropathol. Exp. Neurol. 53*, 158−64.
33. Akiyama, H., Barger, S., Barnum, S., Bradt, B., Bauer, J., Cole, G. M., Cooper, N. R., Eikelenboom, P., Emmerling, M., Fiebich, B. L., Finch, C. E., Frautschy, S., Griffin, W. S., Hampel, H., Hull, M., Landreth, G., Lue, L., Mrak, R., Mackenzie, I. R., McGeer, P. L., O'Banion, M. K., Pachter, J., Pasinetti, G., Plata-Salaman, C., Rogers, J., Rydel, R., Shen, Y., Streit, W., Strohmeyer, R., Tooyoma, I., Van Muiswinkel, F. L., Veerhuis, R., Walker, D., Webster, S., Wegrzyniak, B., Wenk, G., and Wyss-Coray, T. (2000) Inflammation and Alzheimer's disease, *Neurobiol. Aging 21*, 383−421.

34. Forster, M. J., Dubey, A., Dawson, K. M., Stutts, W. A., Lal, H., and Sohal, R. S. (1996) Age-related losses of cognitive function and motor skills in mice are associated with oxidative protein damage in the brain, *Proc. Natl. Acad. Sci. U.S.A. 93*, 4765−9.
35. Hensley, K., Butterfield, D. A., Hall, N., Cole, P., Subramaniam, R., Mark, R., Mattson, M. P., Markesbery, W. R., Harris, M. E., Aksenov, M., et al. (1996) Reactive oxygen species as causal agents in the neurotoxicity of the Alzheimer's disease-associated amyloid β peptide, *Ann. N.Y. Acad. Sci. 786*, 120−34.
36. Smith, C. D., Carney, J. M., Tatsumo, T., Stadtman, E. R., Floyd, R. A., and Markesbery, W. R. (1992) Protein oxidation in aging brain, *Ann. N.Y. Acad. Sci. 663*, 110−9.
37. Smith, C. D., Carney, J. M., Starke-Reed, P. E., Oliver, C. N., Stadtman, E. R., Floyd, R. A., and Markesbery, W. R. (1991) Excess brain protein oxidation and enzyme dysfunction in normal aging and in Alzheimer disease, *Proc. Natl. Acad. Sci. U.S.A. 88*, 10540−3.
38. Hall, E. D., Detloff, M. R., Johnson, K., and Kupina, N. C. (2004) Peroxynitrite-mediated protein nitration and lipid peroxidation in a mouse model of traumatic brain injury, *J. Neurotrauma 21*, 9−20.
39. Kennedy, L. J., Moore, K., Jr., Caulfield, J. L., Tannenbaum, S. R., and Dedon, P. C. (1997) Quantitation of 8-oxoguanine and strand breaks produced by four oxidizing agents, *Chem. Res. Toxicol. 10*, 386−92.
40. Douki, T., and Cadet, J. (1996) Peroxynitrite mediated oxidation of purine bases of nucleosides and isolated DNA, *Free Radical Res. 24*, 369−80.
41. Niles, J. C., Wishnok, J. S., and Tannenbaum, S. R. (2000) A novel nitration product formed during the reaction of peroxynitrite with 2′,3′,5′-tri-O-acetyl-7,8-dihydro-8-oxoguanosine: N-Nitro-N′-[1-(2,3,5-tri-O-acetyl-β-D-erythro-pentofuranosyl)-2,4-dioxoimidazolidin-5-ylidene]guanidine, *Chem. Res. Toxicol. 13*, 390−6.
42. Niles, J. C., Wishnok, J. S., and Tannenbaum, S. R. (2001) A novel nitroimidazole compound formed during the reaction of peroxynitrite with 2′,3′,5′-tri-O-acetyl-guanosine, *J. Am. Chem. Soc. 123*, 12147−51.
43. MacMillan-Crow, L. A., Crow, J. P., and Thompson, J. A. (1998) Peroxynitrite-mediated inactivation of manganese superoxide dismutase involves nitration and oxidation of critical tyrosine residues, *Biochemistry 37*, 1613−22.
44. MacMillan-Crow, L. A., and Thompson, J. A. (1999) Tyrosine modifications and inactivation of active site manganese superoxide dismutase mutant (Y34F) by peroxynitrite, *Arch. Biochem. Biophys. 366*, 82−8.
45. Takakura, K., Beckman, J. S., MacMillan-Crow, L. A., and Crow, J. P. (1999) Rapid and irreversible inactivation of protein tyrosine phosphatases PTP1B, CD45, and LAR by peroxynitrite, *Arch. Biochem. Biophys. 369*, 197−207.
46. Roberts, E. S., Lin, H., Crowley, J. R., Vuletich, J. L., Osawa, Y., and Hollenberg, P. F. (1998) Peroxynitrite-mediated nitration of tyrosine and inactivation of the catalytic activity of cytochrome P450 2B1, *Chem. Res. Toxicol. 11*, 1067−74.
47. Beckman, J. S. (1996) Oxidative damage and tyrosine nitration from peroxynitrite, *Chem. Res. Toxicol. 9*, 836−44.
48. Ischiropoulos, H., Duran, D., and Horwitz, J. (1995) Peroxynitrite-mediated inhibition of DOPA synthesis in PC12 cells, *J. Neurochem. 65*, 2366−72.
49. Coyle, J. T., and Puttfarcken, P. (1993) Oxidative stress, glutamate, and neurodegenerative disorders, *Science 262*, 689−95.
50. Akaike, T., Noguchi, Y., Ijiri, S., Setoguchi, K., Suga, M., Zheng, Y. M., Dietzschold, B., and Maeda, H. (1996) Pathogenesis of influenza virus-induced pneumonia: Involvement of both nitric oxide and oxygen radicals, *Proc. Natl. Acad. Sci. U.S.A. 93*, 2448−53.
51. Beckman, J. S., and Koppenol, W. H. (1996) Nitric oxide, superoxide, and peroxynitrite: The good, the bad, and ugly, *Am. J. Physiol. 271*, C1424−37.
52. Ischiropoulos, H. (2003) Biological selectivity and functional aspects of protein tyrosine nitration, *Biochem. Biophys. Res. Commun. 305*, 776−83.
53. Souza, J. M., Daikhin, E., Yudkoff, M., Raman, C. S., and Ischiropoulos, H. (1999) Factors determining the selectivity of protein tyrosine nitration, *Arch. Biochem. Biophys. 371*, 169−78.
54. Greenacre, S. A., and Ischiropoulos, H. (2001) Tyrosine nitration: Localisation, quantification, consequences for protein function and signal transduction, *Free Radical Res. 34*, 541−81.
55. Guittet, O., Decottignies, P., Serani, L., Henry, Y., Le Marechal, P., Laprevote, O., and Lepoivre, M. (2000) Peroxynitrite-mediated nitration of the stable free radical tyrosine residue of the ribonucleotide reductase small subunit, *Biochemistry 39*, 4640−8.
56. Ara, J., Przedborski, S., Naini, A. B., Jackson-Lewis, V., Trifiletti, R. R., Horwitz, J., and Ischiropoulos, H. (1998) Inactivation of tyrosine hydroxylase by nitration following exposure to peroxynitrite and 1-methyl-4-phenyl-1,2,3,6-tetrahydropyridine (MPTP), *Proc. Natl. Acad. Sci. U.S.A. 95*, 7659−63.
57. Souza, J. M., Giasson, B. I., Chen, Q., Lee, V. M., and Ischiropoulos, H. (2000) Dityrosine cross-linking promotes formation of stable α-synuclein polymers. Implication of nitrative and oxidative stress in the pathogenesis of neurodegenerative synucleinopathies, *J. Biol. Chem. 275*, 18344−9.
58. Atwood, C. S., Perry, G., Zeng, H., Kato, Y., Jones, W. D., Ling, K. Q., Huang, X., Moir, R. D., Wang, D., Sayre, L. M., Smith, M. A., Chen, S. G., and Bush, A. I. (2004) Copper mediates dityrosine cross-linking of Alzheimer's amyloid-β, *Biochemistry 43*, 560−8.
59. Lee, G., Cowan, N., and Kirschner, M. (1988) The primary structure and heterogeneity of tau protein from mouse brain, *Science 239*, 285−8.
60. Goedert, M. (1998) Neurofibrillary pathology of Alzheimer's disease and other tauopathies, *Prog. Brain Res. 117*, 287−306.
61. Kosik, K. S., Orecchio, L. D., Binder, L., Trojanowski, J. Q., Lee, V. M., and Lee, G. (1988) Epitopes that span the tau molecule are shared with paired helical filaments, *Neuron 1*, 817−25.
62. Gamblin, T. C., Berry, R. W., and Binder, L. I. (2003) Tau polymerization: Role of the amino terminus, *Biochemistry 42*, 2252−7.
63. Buee, L., Bussiere, T., Buee-Scherrer, V., Delacourte, A., and Hof, P. R. (2000) Tau protein isoforms, phosphorylation and role in neurodegenerative disorders, *Brain Res. Brain Res. Rev. 33*, 95−130.
64. Gamblin, T. C., Berry, R. W., and Binder, L. I. (2003) Modeling tau polymerization in vitro: A review and synthesis, *Biochemistry 42*, 15009−17.
65. King, M. E., Gamblin, T. C., Kuret, J., and Binder, L. I. (2000) Differential assembly of human tau isoforms in the presence of arachidonic acid, *J. Neurochem. 74*, 1749−57.
66. Novak, M., Kabat, J., and Wischik, C. M. (1993) Molecular characterization of the minimal protease resistant tau unit of the Alzheimer's disease paired helical filament, *EMBO J. 12*, 365−70.
67. Berry, R. W., Abraha, A., Lagalwar, S., LaPointe, N., Gamblin, T. C., Cryns, V. L., and Binder, L. I. (2003) Inhibition of tau polymerization by its carboxy-terminal caspase cleavage fragment, *Biochemistry 42*, 8325−31.
68. Lee, V. M., Goedert, M., and Trojanowski, J. Q. (2001) Neurodegenerative tauopathies, *Annu. Rev. Neurosci. 24*, 1121−59.
69. Reynolds, M. R., Berry, R. W., and Binder, L. I. (2005) Site-Specific Nitration Differentially Influences tau Assembly in Vitro, *Biochemistry 44*, 13997−4009.
70. Goedert, M., Spillantini, M. G., Jakes, R., Rutherford, D., and Crowther, R. A. (1989) Multiple isoforms of human microtubule-associated protein tau: Sequences and localization in neurofibrillary tangles of Alzheimer's disease, *Neuron 3*, 519−26.
71. Reynolds, M. R., Berry, R. W., and Binder, L. I. (2005) Site-Specific Nitration and Oxidative Dityrosine Bridging of the tau Protein by Peroxynitrite: Implications for Alzheimer's Disease, *Biochemistry 44*, 1690−700.
72. Studier, F. W., Rosenberg, A. H., Dunn, J. J., and Dubendorff, J. W. (1990) Use of T7 RNA polymerase to direct expression of cloned genes, *Methods Enzymol. 185*, 60−89.
73. Abraha, A., Ghoshal, N., Gamblin, T. C., Cryns, V., Berry, R. W., Kuret, J., and Binder, L. I. (2000) C-Terminal inhibition of tau assembly in vitro and in Alzheimer's disease, *J. Cell Sci. 113* (Part 21), 3737−45.
74. Beckman, J. S., Chen, J., Ischiropoulos, H., and Crow, J. P. (1994) Oxidative chemistry of peroxynitrite, *Methods Enzymol. 233*, 229−40.
75. Uppu, R. M., Squadrito, G. L., Cueto, R., and Pryor, W. A. (1996) Selecting the most appropriate synthesis of peroxynitrite, *Methods Enzymol. 269*, 285−96.
76. Lowry, O. H., Rosebrough, N. J., Farr, A. L., and Randall, R. J. (1951) Protein measurement with the Folin phenol reagent, *J. Biol. Chem. 193*, 265−75.
77. Ischiropoulos, H., and al-Mehdi, A. B. (1995) Peroxynitrite-mediated oxidative protein modifications, *FEBS Lett. 364*, 279−82.

78. Gamblin, T. C., King, M. E., Dawson, H., Vitek, M. P., Kuret, J., Berry, R. W., and Binder, L. I. (2000) In vitro polymerization of tau protein monitored by laser light scattering: Method and application to the study of FTDP-17 mutants, *Biochemistry 39*, 6136−44.
79. Gamblin, T. C., King, M. E., Kuret, J., Berry, R. W., and Binder, L. I. (2000) Oxidative regulation of fatty acid-induced tau polymerization, *Biochemistry 39*, 14203−10.
80. Williams, R. C., Jr., and Lee, J. C. (1982) Preparation of tubulin from brain, *Methods Enzymol. 85* (Part B), 376−85.
81. Goedert, M., Spillantini, M. G., Cairns, N. J., and Crowther, R. A. (1992) Tau proteins of Alzheimer paired helical filaments: Abnormal phosphorylation of all six brain isoforms, *Neuron 8*, 159−68.
82. Wilson, D. M., and Binder, L. I. (1997) Free fatty acids stimulate the polymerization of tau and amyloid β peptides. In vitro evidence for a common effector of pathogenesis in Alzheimer's disease, *Am. J. Pathol. 150*, 2181−95.
83. King, M. E., Ahuja, V., Binder, L. I., and Kuret, J. (1999) Ligand-dependent tau filament formation: Implications for Alzheimer's disease progression, *Biochemistry 38*, 14851−9.
84. Paxinou, E., Chen, Q., Weisse, M., Giasson, B. I., Norris, E. H., Rueter, S. M., Trojanowski, J. Q., Lee, V. M., and Ischiropoulos, H. (2001) Induction of α-synuclein aggregation by intracellular nitrative insult, *J. Neurosci. 21*, 8053−61.
85. Hiller, G., and Weber, K. (1978) Radioimmunoassay for tubulin: A quantitative comparison of the tubulin content of different established tissue culture cells and tissues, *Cell 14*, 795−804.
86. Levy, S. F., Leboeuf, A. C., Massie, M. R., Jordan, M. A., Wilson, L., and Feinstein, S. C. (2005) Three- and four-repeat tau regulate the dynamic instability of two distinct microtubule subpopulations in qualitatively different manners. Implications for neurodegeneration, *J. Biol. Chem. 280*, 13520−8.
87. Lee, G., Thangavel, R., Sharma, V. M., Litersky, J. M., Bhaskar, K., Fang, S. M., Do, L. H., Andreadis, A., Van Hoesen, G., and Ksiezak-Reding, H. (2004) Phosphorylation of tau by fyn: Implications for Alzheimer's disease, *J. Neurosci. 24*, 2304−12.
88. Yan, S. D., Chen, X., Schmidt, A. M., Brett, J., Godman, G., Zou, Y. S., Scott, C. W., Caputo, C., Frappier, T., Smith, M. A., et al. (1994) Glycated tau protein in Alzheimer disease: A mechanism for induction of oxidant stress, *Proc. Natl. Acad. Sci. U.S.A. 91*, 7787−91.
89. Wang, J. Z., Grundke-Iqbal, I., and Iqbal, K. (1996) Glycosylation of microtubule-associated protein tau: An abnormal posttranslational modification in Alzheimer's disease, *Nat. Med. 2*, 871−5.
90. Bancher, C., Grundke-Iqbal, I., Iqbal, K., Fried, V. A., Smith, H. T., and Wisniewski, H. M. (1991) Abnormal phosphorylation of tau precedes ubiquitination in neurofibrillary pathology of Alzheimer disease, *Brain Res. 539*, 11−8.
91. Iqbal, K., and Grundke-Iqbal, I. (1991) Ubiquitination and abnormal phosphorylation of paired helical filaments in Alzheimer's disease, *Mol. Neurobiol. 5*, 399−410.
92. Morishima, M., and Ihara, Y. (1994) Posttranslational modifications of tau in paired helical filaments, *Dementia 5*, 282−8.
93. Halverson, R. A., Lewis, J., Frausto, S., Hutton, M., and Muma, N. A. (2005) Tau protein is cross-linked by transglutaminase in P301L tau transgenic mice, *J. Neurosci. 25*, 1226−33.
94. Tucholski, J., Kuret, J., and Johnson, G. V. (1999) Tau is modified by tissue transglutaminase in situ: Possible functional and metabolic effects of polyamination, *J. Neurochem. 73*, 1871−80.
95. Horiguchi, T., Uryu, K., Giasson, B. I., Ischiropoulos, H., LightFoot, R., Bellmann, C., Richter-Landsberg, C., Lee, V. M., and Trojanowski, J. Q. (2003) Nitration of tau protein is linked to neurodegeneration in tauopathies, *Am. J. Pathol. 163*, 1021−31.
96. Lee, V. M., Balin, B. J., Otvos, L., Jr., and Trojanowski, J. Q. (1991) A68: A major subunit of paired helical filaments and derivatized forms of normal Tau, *Science 251*, 675−8.
97. Greenberg, S. G., and Davies, P. (1990) A preparation of Alzheimer paired helical filaments that displays distinct tau proteins by polyacrylamide gel electrophoresis, *Proc. Natl. Acad. Sci. U.S.A. 87*, 5827−31.
98. Greenberg, S. G., Davies, P., Schein, J. D., and Binder, L. I. (1992) Hydrofluoric acid-treated tau PHF proteins display the same biochemical properties as normal tau, *J. Biol. Chem. 267*, 564−9.
99. Lu, Q., and Wood, J. G. (1993) Functional studies of Alzheimer's disease tau protein, *J. Neurosci. 13*, 508−15.
100. Yoshida, H., and Ihara, Y. (1993) Tau in paired helical filaments is functionally distinct from fetal tau: Assembly incompetence of paired helical filament-tau, *J. Neurochem. 61*, 1183−6.
101. Kondo, J., Honda, T., Mori, H., Hamada, Y., Miura, R., Ogawara, M., and Ihara, Y. (1988) The carboxyl third of tau is tightly bound to paired helical filaments, *Neuron 1*, 827−34.
102. Morishima-Kawashima, M., Hasegawa, M., Takio, K., Suzuki, M., Titani, K., and Ihara, Y. (1993) Ubiquitin is conjugated with amino-terminally processed tau in paired helical filaments, *Neuron 10*, 1151−60.
103. Horowitz, P. M., Patterson, K. R., Guillozet-Bongaarts, A. L., Reynolds, M. R., Carroll, C. A., Weintraub, S. T., Bennett, D. A., Cryns, V. L., Berry, R. W., and Binder, L. I. (2004) Early N-terminal changes and caspase-6 cleavage of tau in Alzheimer's disease, *J. Neurosci. 24*, 7895−902.
104. Ledesma, M. D., Bonay, P., Colaco, C., and Avila, J. (1994) Analysis of microtubule-associated protein tau glycation in paired helical filaments, *J. Biol. Chem. 269*, 21614−9.
105. Lee, V. M., Wang, J., and Trojanowski, J. Q. (1999) Purification of paired helical filament tau and normal tau from human brain tissue, *Methods Enzymol. 309*, 81−9.
106. Hensley, K., Maidt, M. L., Yu, Z., Sang, H., Markesbery, W. R., and Floyd, R. A. (1998) Electrochemical analysis of protein nitrotyrosine and dityrosine in the Alzheimer brain indicates region-specific accumulation, *J. Neurosci. 18*, 8126−32.
107. Kato, Y., Wu, X., Naito, M., Nomura, H., Kitamoto, N., and Osawa, T. (2000) Immunochemical detection of protein dityrosine in atherosclerotic lesion of apo-E-deficient mice using a novel monoclonal antibody, *Biochem. Biophys. Res. Commun. 275*, 11−5.
108. Goode, B. L., Chau, M., Denis, P. E., and Feinstein, S. C. (2000) Structural and functional differences between 3-repeat and 4-repeat tau isoforms. Implications for normal tau function and the onset of neurodegenetative disease, *J. Biol. Chem. 275*, 38182−9.
109. Makrides, V., Massie, M. R., Feinstein, S. C., and Lew, J. (2004) Evidence for two distinct binding sites for tau on microtubules, *Proc. Natl. Acad. Sci. U.S.A. 101*, 6746−51.
110. Gustke, N., Trinczek, B., Biernat, J., Mandelkow, E. M., and Mandelkow, E. (1994) Domains of tau protein and interactions with microtubules, *Biochemistry 33*, 9511−22.
111. Preuss, U., Biernat, J., Mandelkow, E. M., and Mandelkow, E. (1997) The 'jaws' model of tau-microtubule interaction examined in CHO cells, *J. Cell Sci. 110* (Part 6), 789−800.
112. Goode, B. L., and Feinstein, S. C. (1994) Identification of a novel microtubule binding and assembly domain in the developmentally regulated inter-repeat region of tau, *J. Cell Biol. 124*, 769−82.
113. Cleveland, D. W., Hwo, S. Y., and Kirschner, M. W. (1977) Physical and chemical properties of purified tau factor and the role of tau in microtubule assembly, *J. Mol. Biol. 116*, 227−47.
114. Bramblett, G. T., Goedert, M., Jakes, R., Merrick, S. E., Trojanowski, J. Q., and Lee, V. M. (1993) Abnormal tau phosphorylation at Ser396 in Alzheimer's disease recapitulates development and contributes to reduced microtubule binding, *Neuron 10*, 1089−99.
115. Drechsel, D. N., Hyman, A. A., Cobb, M. H., and Kirschner, M. W. (1992) Modulation of the dynamic instability of tubulin assembly by the microtubule-associated protein tau, *Mol. Biol. Cell 3*, 1141−54.
116. Biernat, J., Gustke, N., Drewes, G., Mandelkow, E. M., and Mandelkow, E. (1993) Phosphorylation of Ser262 strongly reduces binding of tau to microtubules: Distinction between PHF-like immunoreactivity and microtubule binding, *Neuron 11*, 153−63.
117. Feinstein, S. C., and Wilson, L. (2005) Inability of tau to properly regulate neuronal microtubule dynamics: A loss-of-function mechanism by which tau might mediate neuronal cell death, *Biochim. Biophys. Acta 1739*, 268−79.
118. Hyman, B. T., Marzloff, K., Wenniger, J. J., Dawson, T. M., Bredt, D. S., and Snyder, S. H. (1992) Relative sparing of nitric oxide synthase-containing neurons in the hippocampal formation in Alzheimer's disease, *Ann. Neurol. 32*, 818−20.
119. Zhang, Y. J., Xu, Y. F., Chen, X. Q., Wang, X. C., and Wang, J. Z. (2005) Nitration and oligomerization of tau induced by peroxynitrite inhibit its microtubule-binding activity, *FEBS Lett. 579*, 2421−7.

BI052142H